Divergent differentiation paths in airway smooth muscle culture: induction of functionally contractile myocytes

ANDREW J. HALAYKO, BLANCA CAMORETTI-MERCADO, SEAN M. FORSYTHE, JOAQUIM E. VIEIRA, RICHARD W. MITCHELL, MARK E. WYLAM, MARC B. HERSHENSON, AND JULIAN SOLWAY
Section of Pulmonary and Critical Care Medicine, Department of Medicine, University of Chicago, Chicago, Illinois 60637

Halayko, Andrew J., Blanca Camoretti-Mercado, Sean M. Forsythe, Joaquim E. Vieira, Richard W. Mitchell, Mark E. Wylam, Marc B. Hershenson, and Julian Solway. Divergent differentiation paths in airway smooth muscle culture: induction of functionally contractile myocytes. *Am. J. Physiol.* 276 (*Lung Cell. Mol. Physiol.* 20): L197–L206, 1999.—We tested the hypothesis that prolonged serum deprivation would allow a subset of cultured airway myocytes to reacquire the abundant contractile protein content, marked shortening capacity, and elongated morphology characteristic of contractile cells within intact tissue. *Passage 1* or *2* canine tracheal smooth muscle (SM) cells were grown to confluence, then serum deprived for up to 19 days. During serum deprivation, two differentiation pathways emerged. One-sixth of the cells developed an elongated morphology and aligned into bundles. Elongated myocytes contained cables of contractile myofilaments, dense bodies, gap junctions, and membrane caveoli, ultrastructural features of contractile SM in tissue. These cells immunostained intensely for SM α-actin, SM myosin heavy chain (MHC), and SM22 (an SM-specific actin-binding protein), and Western analysis of culture lysates disclosed 1.8 (SM α-actin)-, 7.7 (SM MHC)-, and 5.8 (SM22)-fold protein increases during serum deprivation. Immunoreactive M_3 muscarinic receptors were present in dense foci distributed throughout elongated, SM MHC-positive myocytes. ACh (10^{-3} M) induced a marked shortening (59.7 ± 14.4% of original length) in 62% of elongated myocytes made semiadherent by gentle proteolytic digestion, and membrane bleb formation (a consequence of contraction) occurred in all stimulated cells that remained adherent and so did not shorten. Cultured airway myocytes that did not elongate during serum deprivation instead became short and flattened, lost immunoreactivity for contractile proteins, lacked the M_3 muscarinic-receptor expression pattern seen in elongated cells, and exhibited no contractile response to ACh. Thus we demonstrate that prolonged serum deprivation induces distinct differentiation pathways in confluent cultured tracheal myocytes and that one subpopulation acquires an unequivocally functional contractile phenotype in which structure and function resemble contractile myocytes from intact tissue.

phenotypic modulation; serum deprivation; contraction; ultrastructure; heterogeneity; muscarinic receptors; contractile proteins

IN NORMAL TISSUES, smooth muscle (SM) cells (SMCs) contract to regulate the luminal diameter of hollow organs. In disease states, SMCs also serve as effectors of fibrosis, muscle mass accumulation, and inflammation (13, 24). For example, myocytes of the "synthetic-proliferative" phenotype appear in atherosclerotic lesions and arise from phenotypic modulation of contractile cells and/or selection of preexisting subsets of myocytes that retain these potential functions (14). Synthetic-proliferative myocytes express little contractile apparatus and instead synthesize matrix proteins, growth factors, and cytokines.

Cell culture of SM has advanced the understanding of SM gene transcription (12, 22), pathways regulating proliferation (35), and cytokine and/or growth factor secretion (6). However, study of the contractile function in cultured SMCs has been hampered by their tendency to acquire the synthetic-proliferative phenotype. Contractile protein content increases at confluence, but even such confluent cells differ importantly from contractile myocytes in SM tissue (11). They do not shorten appreciably when stimulated by contractile agonists, and they do not exhibit intracellular calcium responses to muscarinic stimulation (15, 23, 25, 36). Furthermore, they assume a short, spindlelike morphology that is distinct from the elongated, wormlike shape of myocytes freshly isolated from tissue (11, 13). Notably, confluent cultured SMCs exhibit heterogeneity of morphology, contractile and cytoskeletal protein content (2, 17, 33), and mitogen sensitivity (10, 19). Thus, like in intact tissue, SM cultures include myocytes of differing potential for proliferative, secretory, or contractile function.

Based on previous reports (1, 5, 13, 33) that short-term serum deprivation promotes contractile protein gene expression and the heterogeneity of cultured SMCs cited above, we reasoned that prolonged serum withdrawal from confluent passaged airway myocytes might allow a select subset of cells to reacquire the abundant contractile protein content, marked shortening capacity, and elongated morphology characteristic of contractile phenotype cells within intact tissue. We tested this hypothesis using passaged, cultured canine tracheal myocytes and found that striking morphological elongation, contractile protein accumulation, acetylcholine (ACh)-induced intracellular calcium mobilization (21), and ACh-induced shortening occur in a subset of serum-deprived cells.

METHODS

Materials. Collagenase purified from *Clostridium histolyticum* was purchased from GIBCO BRL (Life Technologies, Grand Island, NY). Elastase type IV and Nagarse protease

The costs of publication of this article were defrayed in part by the payment of page charges. The article must therefore be hereby marked "*advertisement*" in accordance with 18 U.S.C. Section 1734 solely to indicate this fact.

type XXVII were purchased from Sigma (St. Louis, MO). Insulin-transferrin-selenium culture medium supplement was obtained from Collaborative Biomedical Products (Bedford, MA). Nonessential amino acid (NEAA) nutrient supplement was purchased from GIBCO BRL (Life Technologies). Monoclonal mouse antibodies used for Western blotting and immunocytochemical studies included anti-SM myosin heavy chain (MHC; clone hSM-V), anti-SM α-actin (clone 1A4), and anti-α-actin (clone AC-74) from Sigma Immunochemicals. Polyclonal guinea pig anti-SM22 was a gift from Dr. W. Gerthoffer (University of Nevada, Reno). Polyclonal rabbit anti-M_2 and anti-M_3 muscarinic-receptor antibodies were purchased from Research and Diagnostic Antibodies (Richmond, CA). Fluorescein isothiocyanate (FITC)-conjugated donkey anti-mouse IgG was obtained from Amersham Life Science (Arlington Heights, IL). FITC-conjugated sheep anti-guinea pig IgG and indocarbocyanine-conjugated goat anti-rabbit IgG were purchased from Jackson ImmunoResearch Laboratories (West Grove, PA).

Canine tracheal SM cultures. Tracheae were obtained from adult mongrel dogs, and primary SMC cultures were established as previously described (11). Briefly, cleaned tracheal muscle was obtained by dissection and minced with scissors. Myocytes were enzymatically dispersed for 60 min at 37°C in buffered saline containing 600 U/ml of collagenase, 10 U/ml of elastase, and 2 U/ml of Nagarse protease. Isolated cells were seeded on uncoated plastic culture plates at a density of $5–10 \times 10^3$ cells/cm^2 in Dulbecco's modified Eagle's medium supplemented with 10% fetal bovine serum, 0.1 mM NEAAs, 50 U/ml of penicillin, and 50 μg/ml of streptomycin. Cells were grown at 37°C in a humidified incubator under 5% CO_2. Cultures were passaged at confluence by lifting the cells with 0.05% trypsin-0.5 mM EDTA and reseeding them into three new culture plates per confluent dish. Cells from *passage 1* or *2* were used in the studies.

To induce phenotypic differentiation of tracheal myocytes, cultured cells were grown to confluence, then serum-containing growth medium was replaced with serum-free Ham's F-12 medium supplemented with insulin-transferrin-selenium medium (final concentrations: 5 μg/ml of insulin, 5 μg/ml of transferrin, and 5 ng/ml of selenium), 0.1 mM NEAAs, 50 U/ml of penicillin, and 50 μg/ml of streptomycin. Fresh serum-free medium was provided every 48–72 h thereafter. Cell morphology was assessed with a Nikon Diaphot II phase-contrast microscope equipped with a 35-mm camera.

Fluorescence immunocytochemistry. Cells were grown as in *Canine tracheal SM cultures* but on precleaned sterile glass coverslips. All staining steps were carried out at 4°C unless otherwise noted. Antibodies were diluted in PBS (pH 7.4) containing 0.1% Tween 20 (PBS-T) and 1% bovine serum albumin (BSA); for negative controls, coverslips were incubated in this buffer containing no primary antibody. Cells were fixed for 20 min in PBS containing 1% paraformaldehyde, then were incubated in PBS containing 1% Triton X-100 for 15 min. The coverslips were blocked for 1 h in PBS-T containing 3% BSA and incubated overnight in primary antibody. Primary antibodies included mouse monoclonal anti-SM MHC diluted 1:50; mouse monoclonal anti-SM α-actin diluted 1:500, guinea pig polyclonal anti-SM22 diluted 1:100, or polyclonal rabbit antibodies specific for either M_2 or M_3 muscarinic-receptor subtypes diluted 1:500. For SM MHC, α-actin, and SM22 detection, the cells were washed in PBS-T, then incubated in FITC-conjugated anti-mouse IgG or FITC-conjugated anti-guinea pig IgG for 2 h at room temperature (RT). Cells that were double immunolabeled for SM MHC and M_2 or M_3 muscarinic receptors were incubated in a secondary antibody cocktail containing both FITC-conjugated anti-mouse IgG and indocarbocyanine-conjugated anti-rabbit IgG. To stain the nuclei, the cells were washed, then incubated for 30–45 s at RT in PBS-T containing either 10 μg/ml of propidium iodide plus 50 μg/ml of RNase A or 10 μg/ml of Hoechst 33342. The coverslips were rinsed in water, then mounted on slides with antifade adhesive (85% glycerol, 1 mM *p*-phenylenediamine, and 100 mM Tris, pH 7.4). The slides were stored at −20°C. Fluorescent immunostaining was assessed with a Nikon microscope equipped with epifluorescence optics and a Photometrics SenSys 12-bit digital video camera. Digitized images were captured with Spectrum imaging software (IP Laboratories, Vienna, VA).

Ultrastructural analysis. For transmission electron microscopy, passaged cells were grown to confluence on Permanox culture plates (Nalge Nunc International, Naperville, IL) and were then serum deprived for 12 days. The cells were fixed onto the plates in PBS (pH 7.4) containing 4% paraformaldehyde plus 1.25% gluteraldehyde. The cells were postfixed with 1% osmium tetroxide, then embedded in LX-112 acrylic medium. Blocks were then prepared from areas where bundles of elongate cells were evident by light microscopy. Ultrathin en face longitudinal and transverse sections were prepared, then mounted onto Formvar-coated grids and further stained with 1% uranyl acetate and lead citrate. Cell ultrastructure was assessed with an electron microscope at an acceleration voltage of 60–80 kV.

Evaluation of cytoplasmic coupling through gap junctions. Myocytes deprived of serum for 7–10 days were bathed in HEPES-buffered Krebs solution containing 10 mM taurine and 0.1% BSA. To determine the degree of functional cell-to-cell cytoplasmic coupling, individual cells were microinjected at RT with buffer (40 mM NaCl and 50 mM HEPES, pH 7.4) containing 2% sulforhodamine 101 plus 1% FITC-conjugated 10-kDa dextran. Microinjections were performed during phase-contrast microscopy on a Leica DM-IRB/E epifluorescence microscope equipped with an Eppendorf transjector system; injection duration was 0.6 s, and injection pressure was 80 hPa. Five to seven minutes after injection, rhodamine and fluorescein fluorescences were recorded with a video camera (Optronics Engineering, Goleta, CA) and a Sony video printer.

Western analysis. Temporal changes in the protein composition of cultured cells were assessed by Western analysis as previously described (11). At 0–19 days after initiation of serum deprivation, myocyte cultures were washed with PBS, then total protein homogenates were prepared in extraction buffer that consisted of 0.3% sodium dodecyl sulfate (SDS), 50 mM Tris (pH 7.6), 0.6 M β-mercaptoethanol, 20 μg/ml of leupeptin, 250 μM phenylmethylsulfonyl fluoride, and 50 mg/ml of soybean trypsin inhibitor. Protein lysates (7 μg/lane) were size fractionated by SDS-polyacrylamide gel electrophoresis and then were electroblotted onto nitrocellulose membranes with a semidry transfer. The blots were blocked overnight at 4°C with 3% nonfat milk in Tris-buffered saline (pH 7.4) containing 0.1% Tween 20 (TBS-T). Blots were then incubated for 2–4 h at RT with the primary antibodies diluted in TBS-T with 1% dry milk. The same antibodies used for immunocytochemistry were used for immunoblot analysis of contractile apparatus proteins. In addition, a mouse monoclonal anti-α-actin primary antibody was employed. The blots were incubated for 40 min at RT with either biotinylated sheep anti-mouse IgG or biotinylated sheep anti-guinea pig IgG diluted (1:1,000) in TBS-T. Streptavidin-horseradish peroxidase (1:5,000) in TBS-T was used in the tertiary incubation. Immunoreactive bands were detected on Hyperfilm-ECL using enhanced chemiluminescence reagents (Amersham Life Sciences). To assess the relative abundance of

individual proteins from the resulting chemilumigrams, a Hewlett-Packard scanner with Scanplot software system was used (34).

Contraction of serum-deprived tracheal myocytes. Cultures were grown to confluence in plastic dishes and maintained for 6–10 days in serum-free medium as in *Canine tracheal SM cultures*. All subsequent steps were carried out at RT. The cells were washed twice with Hanks' balanced salt solution containing 10 mM taurine, 1% BSA, and 1 mM dithiothreitol, then incubated for 40–70 min in the presence of 400 units/ml of collagenase and 10 units/ml of papain, to loosen, although not detach, myocytes from the substrata. The cells were washed twice, then incubated in HEPES-buffered Krebs-Henseleit (HKH) solution containing 10 mM taurine and 1% BSA. Semiadherent, elongated myocytes were visualized by phase-contrast microscopy with a Leica DM-IRB/E phase-contrast microscope with video camera and recorder. Individual elongated myocytes were stimulated to contract as follows. A micropipette filled with ACh (10^{-3} M in HKH solution) was positioned within 10 μm of the target cell with an Eppendorf micromanipulator/transjector system. Ach was "puffed" along the cell surface from the micropipette for up to 15 s, and cell shortening was recorded on videotape. To confirm that contractile shortening responses (see *Contraction of serum-deprived tracheal myocytes*) were the direct result of ACh stimulation, atropine (10^{-7} M) was added to some cultures before ACh exposure. In addition, the response of cells puffed with HKH solution alone (i.e., without ACh) were recorded. Cell shortening was measured as the percent change from the original length with National Institutes of Health Image software.

RESULTS

Morphological changes of serum-deprived confluent cultured canine tracheal myocytes. At confluence, canine tracheal myocyte cultures exhibited a typical hill-and-valley appearance (5, 20) characteristic of confluent SMCs growing in serum (Fig. 1*A*). Individual cells assumed a flattened, spindle, or oblong shape, and elongated or worm-shaped cells were very rarely seen. With serum deprivation, though, individual unflattened elongated cells became evident, usually by *day 4* of serum withdrawal, and the hill-and-valley appearance of the cultures was lost. The fraction of individual elongate cells was estimated by counting cells in five ×100 phase-contrast fields from each of four different cultures deprived of serum for 7 days. Elongated morphology was seen in 17.3 ± 8.6% (SD) of the cells. Furthermore, elongated cells tended to appear in parallel and end to end, forming a multilayered pattern of elongated cell bundles up to eight cells wide that coursed randomly through the culture plate (Fig. 1, *B* and *C*). The myocytes that did not become elongate with serum deprivation became very flattened and rather circular and were oriented randomly into a continuous monolayer.

Immunocytochemical analysis of contractile apparatus protein expression. Immunostaining patterns were markedly different at confluence and after 10 days of serum deprivation (Fig. 2). At confluence ("*day 0*" of serum deprivation), virtually all canine tracheal myocytes exhibited weak immunoreactivity for SM α-actin, SM MHC, and SM22 (an SM-specific actin-binding protein). Occasional spindle-shaped cells exhibited stronger immunostaining for α-actin or SM MHC (Fig. 2, *A* and *D*). Cells that stained strongly for α-actin were counted in five ×100 fields on each of three coverslips from three different *day 0* cultures (45 fields total); they comprised only 0.9 ± 0.5% of the total cell population. In marked contrast, serum-deprived myocytes exhibited a much more heterogeneous muscle protein expression. Elongated cells demonstrated strikingly positive immunoreactivity for all three muscle proteins studied, whereas the flattened, circular cells showed virtually no immunoreactivity for these proteins (Fig. 2). α-Actin-positive, elongated myocytes were counted in five ×100 fields from each of three coverslips from three different cultures; after 7 and 14 days of serum deprivation, they comprised 15.2 ± 2.3 and 18.8 ± 5.9%, respectively, of all cells. These data are similar in value to those obtained by counting elongated cells under phase contrast after 7 days of serum deprivation. Thus the fraction of elongated, α-actin-positive cells appears stable by 7 days of serum deprivation. In elongated cells, SM α-actin (Fig. 2*C*), SM MHC (Fig. 2*F*), and SM22 (Fig. 2*I*) appeared primarily along stress fibers or in thick cables oriented parallel to the long axis of the cells. In addition, occasional myocytes of semielongated morphology and moderate muscle protein abundance, similar to the more immunoreactive cells seen in *day 0* cultures, were observed in serum-deprived cultures. Negative control slides incubated only in secondary antibody showed no appreciable staining (data not shown).

Ultrastructural features of serum-deprived cultured canine tracheal myocytes. Transmission electron micrographs (×7,000–40,000 initial magnification) revealed

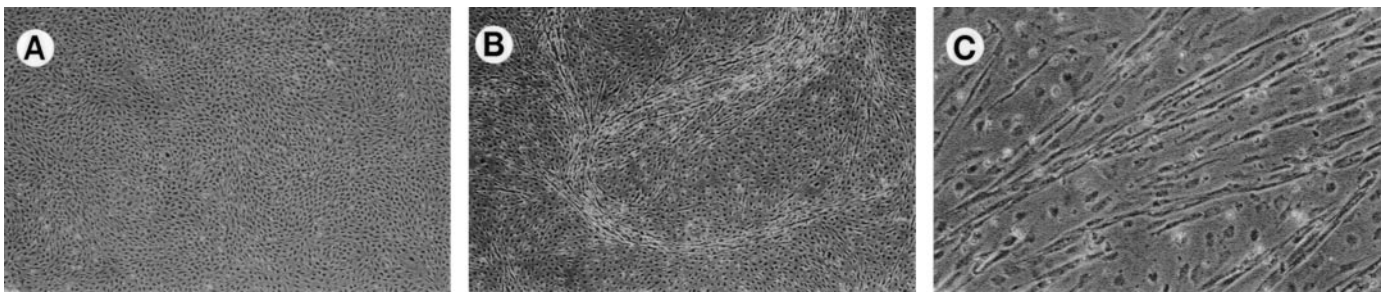

Fig. 1. Phase-contrast micrographs demonstrating typical appearance of confluent (*A*) and 11-day serum-deprived (*B* and *C*) *passage 1* canine tracheal myocytes in primary culture. *A* and *B*: initial magnification, ×40. *C*: initial magnification, ×200.

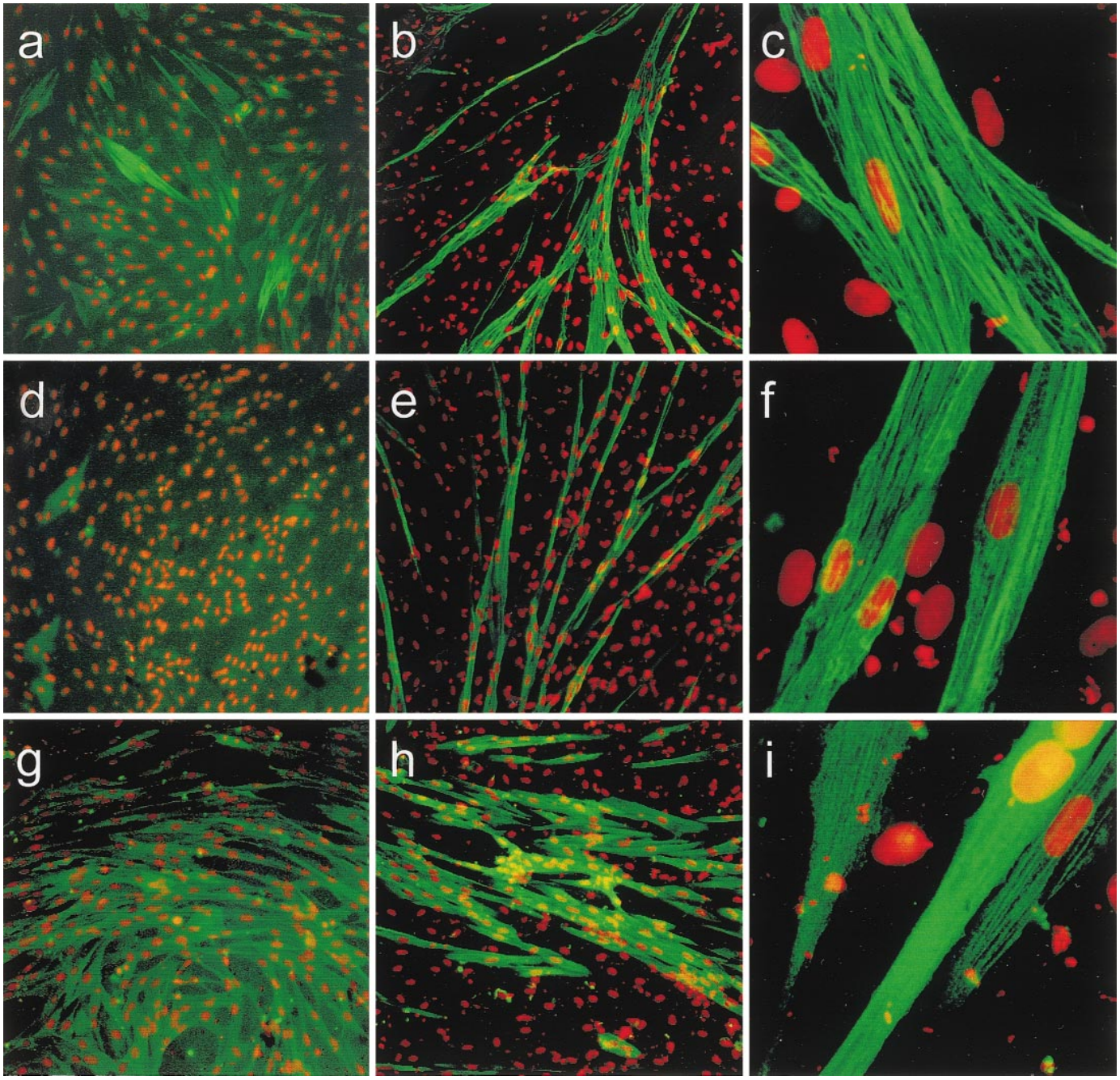

Fig. 2. Fluorescence immunocytochemical staining of cultured *passage 1* canine tracheal myocytes at confluence and after 10 days of serum deprivation. *A*, *D*, and *G*: confluent *day 0* cells at initial magnification of ×100. *B*, *E*, and *H*: 10-day serum-deprived myocytes at initial magnification of ×100. *C*, *F*, and *I*: 10-day serum-deprived myocytes at initial magnification of ×400. *A–C*: anti-smooth muscle α-actin antibody. *D–F*: smooth muscle myosin heavy chain antibody. *G–I*: SM22 antibody. Nuclei were stained with propidium iodide and appear red. Specific primary antibodies, in conjunction with FITC-conjugated secondary antibodies, were used to stain intracellular proteins, which appear green.

that elongated myocytes exhibited ultrastructural features typical of mature, contractile SMCs in tissue (4, 11, 20). As shown in Fig. 3*A*, elongated cells contained large cytoplasmic cables of contractile myofilaments, with characteristic electron-dense structures scattered through the cables. These dense structures likely represent dense bodies as found in SM tissue. Between the contractile filament cables, the cytoplasm contained numerous mitochondria. Typical of SMCs of the contractile phenotype (32), many caveoli were evident along the cell surface membrane (Fig. 3*C*); they often organized into linear arrays of 6–12. Intercellular contacts between elongated cells were predominantly zonae adherens, and a few typical gap junctions were observed (Fig. 3, *D* and *E*). In addition, transverse sections revealed that bundles of elongate cells were

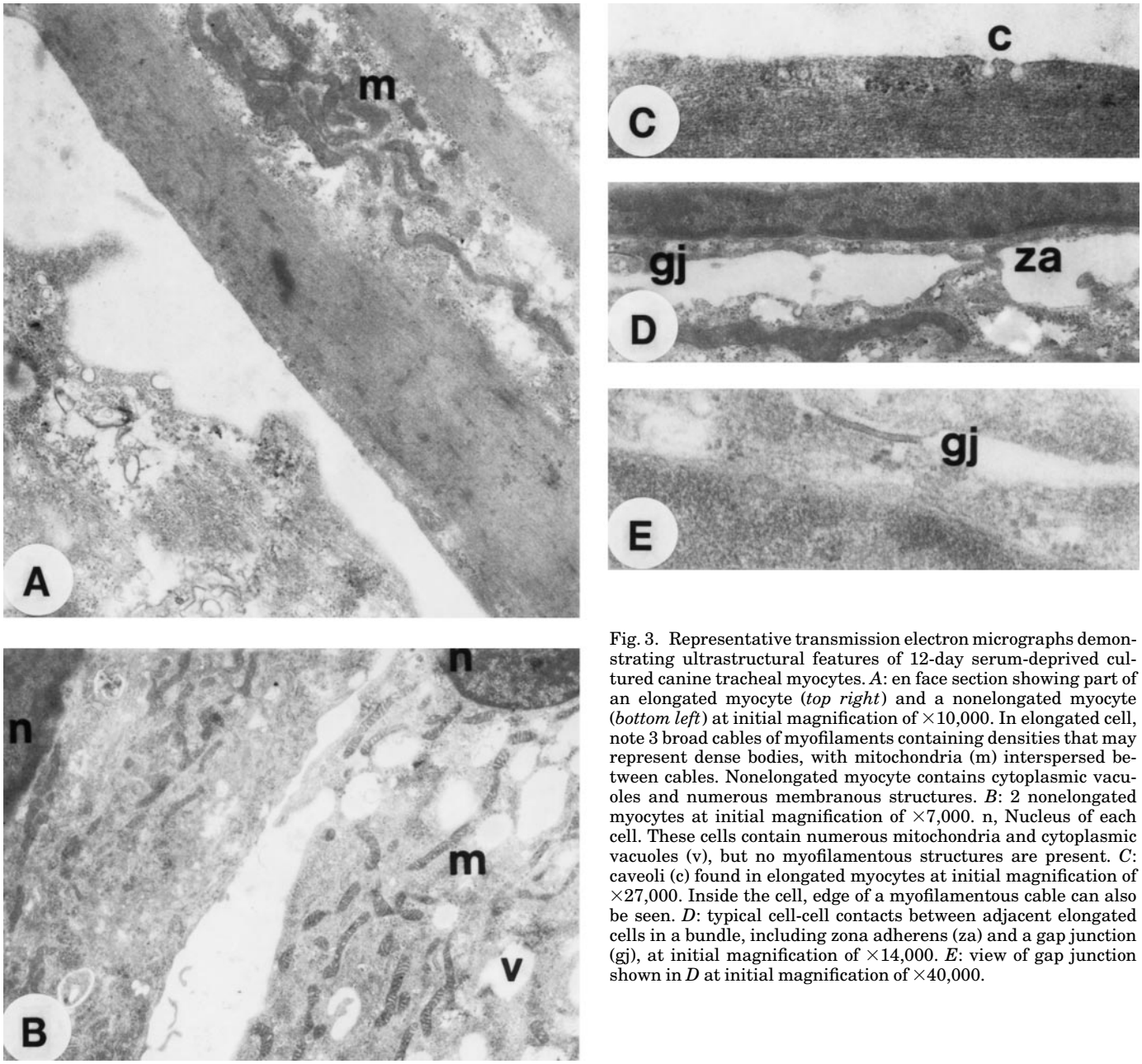

Fig. 3. Representative transmission electron micrographs demonstrating ultrastructural features of 12-day serum-deprived cultured canine tracheal myocytes. *A*: en face section showing part of an elongated myocyte (*top right*) and a nonelongated myocyte (*bottom left*) at initial magnification of ×10,000. In elongated cell, note 3 broad cables of myofilaments containing densities that may represent dense bodies, with mitochondria (m) interspersed between cables. Nonelongated myocyte contains cytoplasmic vacuoles and numerous membranous structures. *B*: 2 nonelongated myocytes at initial magnification of ×7,000. n, Nucleus of each cell. These cells contain numerous mitochondria and cytoplasmic vacuoles (v), but no myofilamentous structures are present. *C*: caveoli (c) found in elongated myocytes at initial magnification of ×27,000. Inside the cell, edge of a myofilamentous cable can also be seen. *D*: typical cell-cell contacts between adjacent elongated cells in a bundle, including zona adherens (za) and a gap junction (gj), at initial magnification of ×14,000. *E*: view of gap junction shown in *D* at initial magnification of ×40,000.

composed of up to six cell layers. In marked contrast, contractile filament cables, dense bodies, and caveoli were absent from nonelongated serum-deprived myocytes, which instead contained numerous mitochondria and cytoplasmic vacuoles and grew as a monolayer (Fig. 3*B*).

Evaluation of cell-cell cytoplasmic coupling. To test whether the gap junctions found in elongated, serum-deprived myocytes by electron microscopy resulted in cell-cell cytoplasmic coupling, we microinjected individual cells with both a small-molecular-mass (606.7 Da), rapidly diffusible marker (sulforhodamine 101) and a large (10-kDa) nondiffusible marker (FITC-conjugated dextran). As shown in Fig. 4, microinjection of a single elongated cell labeled only that cell with nondiffusible fluorescent dextran, but sulforhodamine quickly diffused into three adjacent cells; when present, coupling with two to five cells was typically observed. However, this finding was inconstant in that cytoplasmic coupling with adjacent cells was present in only 6 of the 10 elongated cells so studied. Nonelongated cells also demonstrated sporadic cell-cell cytoplasmic coupling.

Western analysis of muscle protein expression. Western analysis of culture lysates revealed substantial accumulation of SM MHC and SM22 during serum deprivation that reached a plateau after 12 days (Fig. 5). When normalized to the quantity present at confluence (*day 0*), SM MHC and SM22 exhibited the greatest relative increases; the abundance of SM MHC and SM22 was increased significantly in lysates collected after 8 days of serum deprivation ($P < 0.05$ by ANOVA

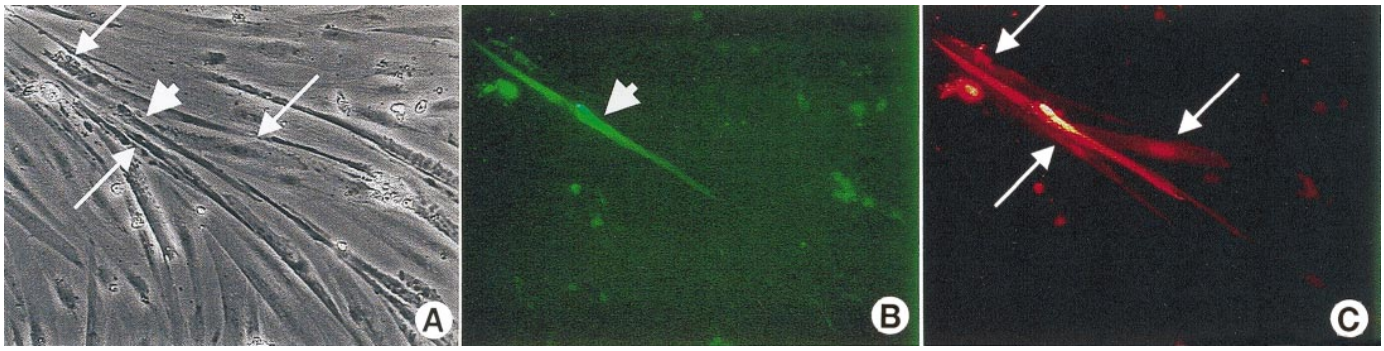

Fig. 4. Cell-cell cytoplasmic coupling between elongated myocytes in serum-deprived canine tracheal smooth muscle cultures. In this typical example, a single elongated myocyte (*A*, thick arrowhead; phase-contrast image) was microinjected with FITC-labeled 10-kDa dextran+sulforhodamine 101. Thin arrows, 3 adjacent cells. Nondiffusible FITC-dextran remained confined to individual cell injected (*B*, arrow; FITC image). In contrast, within 5 min after injection, diffusible sulforhodamine 101 appeared in both injected cell and 3 adjacent cells (*C*, thin arrows; rhodamine image). Lack of FITC-dextran in adjacent cells indicates that sulforhodamine diffused through functional intercellular connections. Both FITC and rhodamine images were obtained ~5 min after microinjection.

and Fisher's least significant difference test). The relatively smaller increase in SM α-actin (<2.3-fold; $P < 0.05$ by ANOVA and Fisher's least significant difference test) likely reflects its greater initial concentration in confluent cells before serum deprivation (Fig. 5; Ref. 11). Given that the elongated cells contain most, if not all, of these muscle proteins in serum-deprived cultures (Fig. 2), the relative increases in mixed culture lysates shown in Fig. 5 represent an underestimation of the changes in protein content within elongated myocytes. In contrast to these increasing muscle-specific protein contents, β-actin abundance in culture lysates remained constant throughout serum deprivation ($P > 0.75$ by ANOVA; Fig. 5).

Contraction of serum-deprived tracheal myocytes. Detachment of elongated cells from the substrata and striking contraction were observed in 62.3% of all elongated cells treated with ACh ($n = 77$ cells from 3 different cultures; Fig. 6*A*). These cells shortened by an average of 59.7 ± 14.4% from the original adherent myocyte length, and most cells shortened by 60–80% (Fig. 6*B*). The duration of shortening was variable and appeared to be dependent on the degree of myocyte attachment to the substratum and contiguous cells. No reelongation of shortened myocytes was seen up to 10 min after maximal contraction was reached. In all serum-deprived elongated myocytes that did not shorten, membrane blebs developed immediately after the first puffs of ACh were received (Fig. 6*C*). The formation of ACh-induced membrane blebs and myocyte shortening was completely inhibited in cells preincubated with atropine, indicating that ACh-induced contractions resulted directly from muscarinic receptor-mediated signaling. In addition, none of the 10 elongated myocytes that were puffed with HKH solution alone showed either of the above indications of contraction. Thus the ACh-induced contractions observed cannot be attributed to any mechanical effect of the puff. Nonelongated myocytes exhibited no morphological response to ACh exposure.

Expression of muscarinic-receptor subtypes. M_2 muscarinic receptors were ubiquitously expressed on myocytes in confluent cultures before serum deprivation and on myocytes of both elongated SM MHC-positive and flattened SM MHC-negative phenotypes in serum-deprived cultures (Fig. 7). In marked contrast, M_3 muscarinic-receptor expression changed markedly after serum deprivation. M_3 muscarinic receptors were prominently expressed in dense foci distributed throughout elongated SM MHC-positive myocytes in serum-deprived cultures (Fig. 7); such foci were distinctly absent from flattened SM MHC-negative cells in serum-deprived cultures and from myocytes from confluent, serum-fed cultures (Fig. 7). Interestingly, minor M_3 muscarinic-receptor immunoreactivity was uniformly present in a polar, perinuclear region in all myocytes under each condition.

DISCUSSION

In this study, we demonstrate the induction of an unequivocally functional contractile phenotype in a distinct, stable subpopulation of cultured, passaged tracheal SMCs. These myocytes express salient features of contractile cells normally present in intact airway tissue including *1*) elongated cellular morphology; *2*) a high intracellular abundance of contractile apparatus-associated proteins; *3*) characteristic ultrastructural features including myofilaments, caveoli, and cytoplasmic dense bodies; *4*) pharmacomechanically coupled M_3 muscarinic surface receptors; and *5*) contraction and marked cell shortening on ACh exposure. Prior studies (11, 13, 28–31) have shown that growth to confluence, serum withdrawal, manipulation of underlying matrix proteins, or cyclic deformational strain can partially skew cultured airway SMCs toward the contractile phenotype. However, no prior study has demonstrated the thorough reconstitution of contractile myocyte morphology, ultrastructure, and function reported here. Furthermore, our observation that only a small subset of cultured airway SMCs follows this differentiation pathway on serum deprivation is novel and discloses remarkable heterogeneity as a characteristic feature of these cells in culture. Ma et al. (18) have

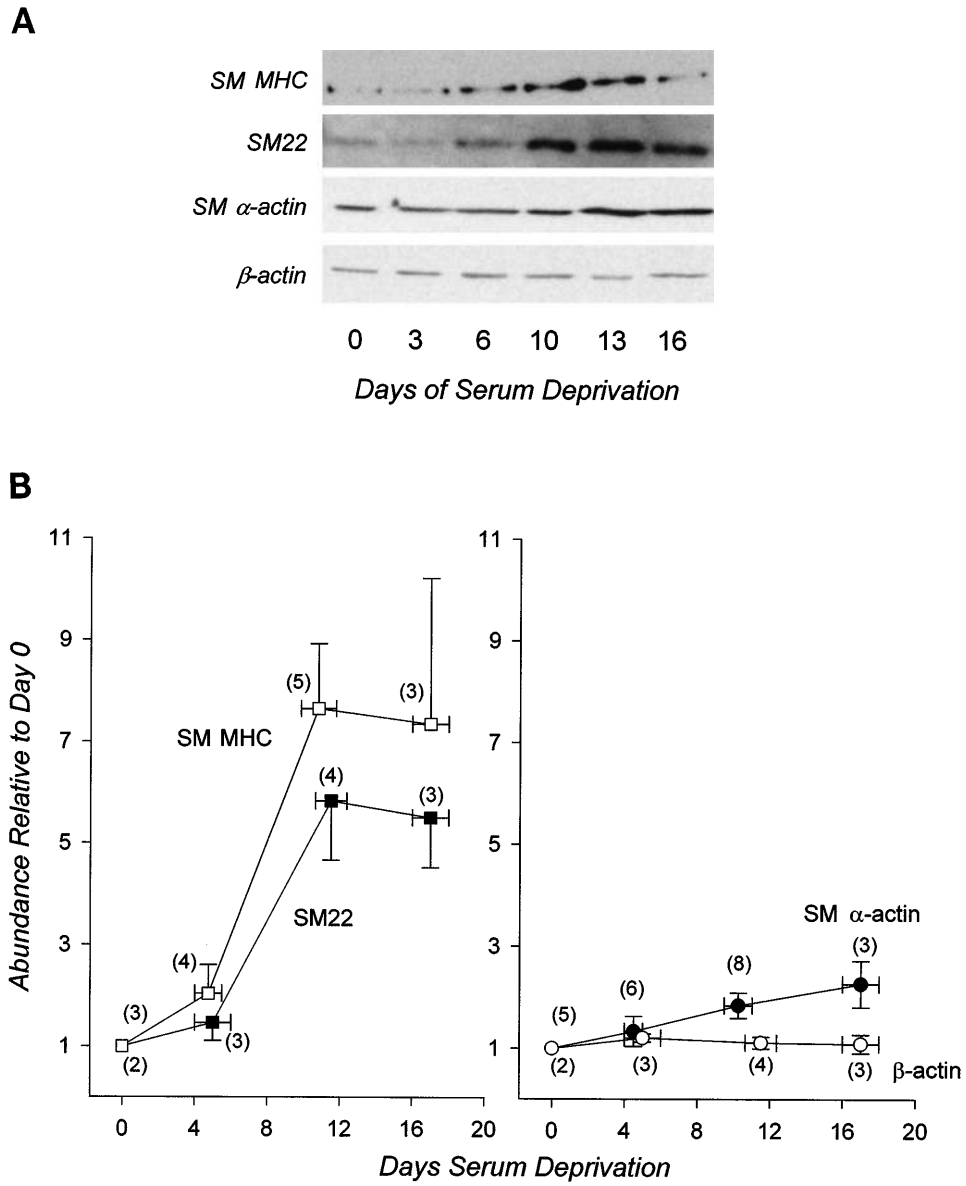

Fig. 5. Western blot analysis of protein expression in passaged canine tracheal myocytes at confluence (*day 0*) and during up to 19 days of subsequent serum deprivation. *A*: Western blots showing smooth muscle (SM) myosin heavy chain (MHC), SM22, SM α-actin, and β-actin. *B*: quantification of changes in protein abundance of SM MHC and SM22 (*left*) and SM α-actin and β-actin (*right*) in culture lysates normalized to level at confluence (*day 0* of serum deprivation). Data from cultures deprived of serum for 3–6, 8–13, or 16–19 days are grouped. Values are means ± SE; nos. in parentheses, no. of cultures analyzed at each point.

just reported similar findings in experiments that parallel the studies reported here.

The morphological, ultrastructural, and biochemical changes that occur when contractile phenotype SMCs modulate toward the synthetic-proliferative phenotype have been well documented (5, 8, 11). In contrast, the factors that orchestrate maturation and coordinated cytostructural remodeling of noncontractile myocytes into functionally contractile SMCs are relatively unexplored. Smith and colleagues (28–30) demonstrated that cyclic stretch of cultured airway SMCs in serum-containing medium partially restored contractile features. Cyclic stretch induced myocyte elongation and alignment perpendicular to the direction of strain, increased numbers of actin stress fibers and focal adhesions, and accumulation of contractile apparatus-associated proteins. Boerth et al. (3) reported that stable transfection of rat aortic SMCs with a gene encoding catalytically active cGMP-dependent protein kinase induced myocyte elongation and partially restored contractile protein content to the levels in intact tissues. Schuger et al. (26), using attached organotypic cultures from embryonic mouse lungs, observed that elongated, contractile protein-rich SMCs differentiate from mesenchymal cells, and some align in concentric layers around epithelial cysts. Similar changes in SM were observed in peribronchial mesenchymal cells during bronchial SMC differentiation in cultured embryonic mouse lung explants (27). Epithelial-mesenchymal contact via basement membranes rich in laminin-α1 was an important determinant of this rearrangement. Our findings confirm the association between acquisition of the contractile phenotype and cytostructural remodeling. However, our results also show that a subset of airway SMCs can acquire a functionally contractile state and can realign into organized cell clusters, even in the absence of external physical stimuli or the paracrine influence of other cell types. Thus it appears that airway SMCs can independently orchestrate myocyte differentiation, phenotypic

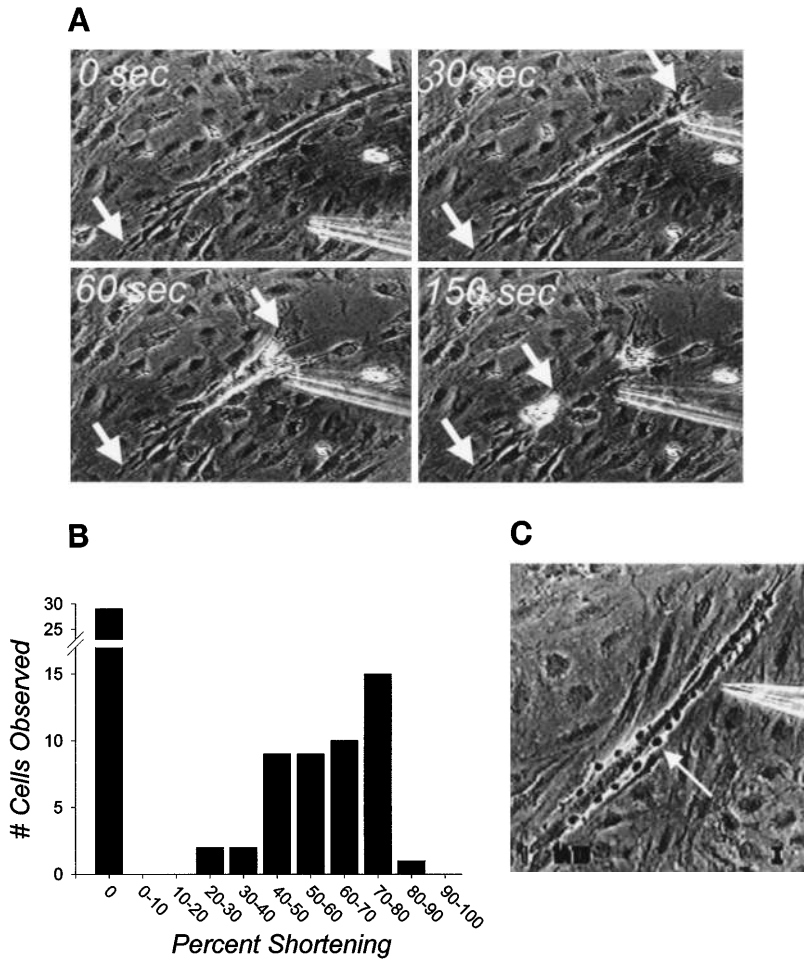

Fig. 6. ACh-induced contraction of elongated cells in serum-deprived canine tracheal myocyte cultures. *A*: example of a typical time course of contraction of an individual semiadherent elongated myocyte. Arrows, position of ends of contracting cell. Cell shown shortened by 74.1% of original adherent myocyte length after ACh exposure. Original magnification, ×100. *B*: distribution of extent of contractile shortening for 77 individual elongated cells induced by stimulation with ACh. *C*: example of prominent membrane bleb formation (arrow) in an elongated myocyte after ACh stimulation. Original magnification, ×200.

expression, and arrangement of cells into organized units.

Our findings confirm and extend accumulating evidence that airway SMCs are heterogeneous both in vivo (7, 9) and in culture (2, 10, 17). Acutely dissociated tracheal or bronchial SMCs include myocytes with a wide range of cell size, contractile protein content, nuclear ploidy, and proliferative potential (9). Heteroge-

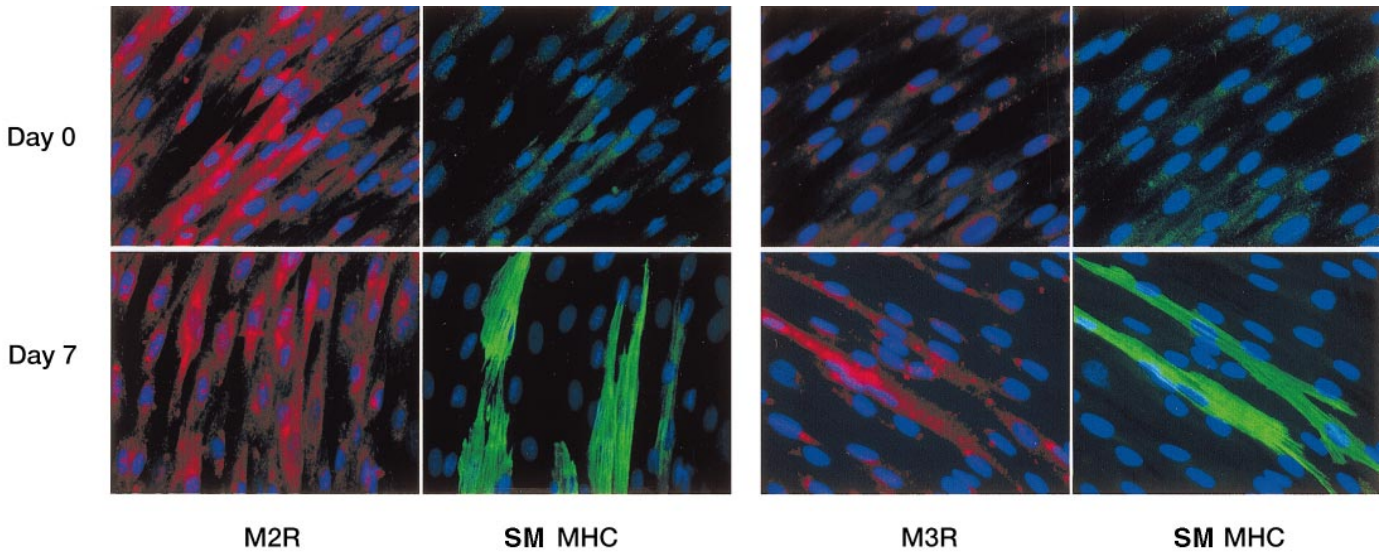

Fig. 7. Double-fluorescence immunocytochemical staining of cultured *passage 1* canine tracheal myocytes at confluence (*day 0*) or after 7 days of serum deprivation (*day 7*). Nuclei were stained with Hoechst 33342 and appear blue. M_2 and M_3 muscarinic receptors (M2R and M3R, respectively) were stained with indocarbocyanine-conjugated secondary antibodies and appear red. SM MHC was stained with FITC-conjugated secondary antibodies and appears green. Original magnification, ×200.

neity among cultured airway myocytes is not well understood, but these cells are known to vary in their sensitivity to mitogens and to the growth-inhibitory influence of heparin (9, 10). Here, we show that only a distinct subset of tracheal myocytes acquires a functionally contractile phenotype during prolonged serum withdrawal. Both the number of contractile phenotype myocytes and their contractile protein content increase no further after 7 days of serum deprivation, reflecting stability of the two subpopulations identified. Thus cultured airway SMCs are heterogeneous not only with respect to their proliferative potential but also in their capacity to coordinate the expression of that complement of genes that renders them functionally contractile. It is important to note that those myocytes that do not elongate and instead become flattened during serum deprivation still remain viable. They remain attached to culture substrata, they contain intracellular organelles of normal appearance, and they synthesize DNA in response to serum restimulation (8). Thus we believe they represent cells modulated toward the synthetic-proliferative phenotype.

Our results also disclose phenotype-specific cellular localization of M_3 muscarinic receptors. M_3 muscarinic receptors appeared in prominent foci along the surface of contractile phenotype, SM MHC-positive myocytes in serum-deprived cultures. In contrast, flattened, SM MHC-negative serum-deprived myocytes, as well as confluent, serum-fed myocytes, demonstrated only polar, perinuclear staining. This striking disparity in M_3 muscarinic-receptor cellular localization, as well as differences in contractile apparatus protein content, may contribute to the divergence of contractile responses to ACh observed in elongated versus flattened serum-deprived myocytes. Serum-fed SMCs do not generate inositol trisphosphate on ACh stimulation (36), and our flattened, noncontractile serum-deprived myocytes do not exhibit ACh-induced increases in intracellular free ionized calcium (21). Thus, even though perinuclear M_3 muscarinic receptors are present in these myocytes, it seems that they do not generate intracellular signals associated with contraction. Apparently, their transport to the cell surface and coupling to intracellular second messengers only occurs in myocytes undergoing modulation to the fully contractile, elongated phenotype. The consistent intracellular distribution of M_2 muscarinic receptors in myocytes under all conditions studied contrasts markedly with the phenotype-specific localization of M_3 muscarinic receptors and underscores the likely importance of M_3 muscarinic-receptor cellular redistribution during contractile phenotype modulation.

In our experiments, elongated SMCs were stimulated to contract while still semiadherent to the culture substratum. This approach allows for a simple and obvious determination of the presence or absence of ACh-induced contraction, but it precludes a precise determination of the unloaded velocity of shortening because an external load is imposed by contiguous cells and matrix interactions. Even so, the extent of shortening observed in most of the contractile cells that did pull free of substratum adhesions was considerably greater than that reported for acutely dissociated airway myocytes (16). Furthermore, we did not observe spontaneous reelongation after contraction as occurs in acutely dispersed cells (16). Together, these findings suggest that the internal elastic load against shortening within our cultured contractile cells may be smaller than that of myocytes acutely dispersed from tissue. Alternatively, differential effects of dissociation enzymes on cultured myocytes and those dissociated from tissue might instead account for the observed differences in shortening and responsiveness. Either of these possibilities could explain the increased velocity of shortening in similarly cultured tracheal myocytes recently described by Ma et al. (18).

Our results raise additional broad questions for which further study seems warranted. These include *1*) what are the transcriptional, translational, and posttranslational regulatory mechanisms that control the marked accumulation of contractile apparatus proteins in serum-deprived tracheal myocytes; *2*) what regulates intracellular localization of muscarinic receptors in airway myocytes; *3*) what underlying factors (internal or external) lead to the distinct differentiation pathways followed by elongated or nonelongated myocytes during serum deprivation, and are these pathways reversible; *4*) how is cellular elongation accomplished in the absence of externally applied forces, and what is the relationship of this process to normal smooth muscle development during embryogenesis; and *5*) why do individual elongated cells appear to align into bundles? The answers to these questions will no doubt identify additional important aspects of airway SM biology.

We thank Dr. W. Gerthoffer (University of Nevada, Reno) for the generous gift of the anti-SM22 antibody.

This work was supported by National Heart, Lung, and Blood Institute Specialized Center of Research Grants HL-56399 and HL-54685; Inspiraplex; Merck-Frosst Canada; Sprague Memorial Institute; the American Lung Association of Metropolitan Chicago; and the American Heart Association of Chicago.

Address for reprint requests: J. Solway, Section of Pulmonary and Critical Care, Dept. of Medicine, Univ. of Chicago, 5841 S. Maryland Ave., MC 6026, Chicago, IL 60637.

Received 29 May 1998; accepted in final form 13 October 1998.

REFERENCES

1. **Blank, R. S., M. M. Thompson, and G. K. Owens.** Cell cycle versus density dependence of smooth muscle alpha actin expression in cultured rat aortic smooth muscle cells. *J. Cell Biol*. 107: 299–306, 1988.
2. **Bochaton-Piallat, M. L., P. Ropraz, F. Gabbiani, and G. Gabbiani.** Phenotypic heterogeneity of rat arterial smooth muscle cell clones. Implications for the development of experimental intimal thickening. *Arterioscler. Thromb. Vasc. Biol*. 16: 815–820, 1996.
3. **Boerth, N. J., N. B. Dey, T. L. Cornwell, and T. M. Lincoln.** Cyclic GMP-dependent protein kinase regulates vascular smooth muscle cell phenotype. *J. Vasc. Res*. 34: 245–259, 1997.
4. **Campbell, J. H., and G. R. Campbell.** Chemical stimuli of the hypertrophic response of smooth muscle. In: *Hypertrophic Response in Smooth Muscle,* edited by C. L. Siedel. Boca Raton, FL: CRC, 1987, p. 153–192.
5. **Chamley-Campbell, J. H., G. R. Campbell, and R. Ross.** The smooth muscle cell in culture. *Physiol. Rev*. 59: 1–61, 1979.
6. **Elias, J. A., Y. Wu, T. Zheng, and R. Panettieri.** Cytokine- and virus-stimulated airway smooth muscle cells produce IL-11 and

other IL-6-type cytokines. *Am. J. Physiol*. 273 (*Lung Cell. Mol. Physiol*. 17): L648–L655, 1997.

7. **Frid, M. G., E. C. Dempsey, A. G. Durmowicz, and K. R. Stenmark.** Smooth muscle cell heterogeneity in pulmonary and systemic vessels. Importance in vascular disease. *Arterioscler. Thromb. Vasc. Biol*. 17: 1203–1209, 1997.
8. **Halayko, A. J., B. Camoretti-Mercado, S. M. Forsythe, J. E. Vieira, Q. Niu, S. Shapiro, M. B. Hershenson, N. L. Stephens, and J. Solway.** Demonstration that individual airway myocytes modulate between contractile and proliferative states in culture (Abstract). *Am. J. Respir. Crit. Care Med*. 157: A747, 1998.
9. **Halayko, A. J., E. Rector, and N. L. Stephens.** Characterization of molecular determinants of smooth muscle cell heterogeneity. *Can. J. Physiol. Pharmacol*. 75: 917–929, 1997.
10. **Halayko, A. J., E. Rector, and N. L. Stephens.** Airway smooth muscle cell proliferation: characterization of subpopulations by sensitivity to heparin inhibition. *Am. J. Physiol*. 274 (*Lung Cell. Mol. Physiol*. 18): L17–L25, 1998.
11. **Halayko, A. J., H. Salari, X. Ma, and N. L. Stephens.** Markers of airway smooth muscle cell phenotype. *Am. J. Physiol*. 270 (*Lung Cell. Mol. Physiol*. 14): L1040–L1051, 1996.
12. **Hautmann, M. B., C. S. Madsen, and G. K. Owens.** A transforming growth factor β (TGF β) control element drives TGF β-induced stimulation of smooth muscle α-actin gene expression in concert with two CArG elements. *J. Biol. Chem*. 272: 10948–10956, 1997.
13. **Hirst, S. J.** Airway smooth muscle cell culture: application to studies of airway wall remodeling and phenotype plasticity in asthma. *Eur. Respir. J*. 9: 808–820, 1996.
14. **Holifield, B., T. Helgason, S. Jamelka, A. Taylor, S. Navran, J. Allen, and C. Siedel.** Differentiated vascular myocytes: are they involved in neointimal formation? *J. Clin. Invest*. 97: 814–825, 1996.
15. **Jain, M., D. Berger, B. Camoretti-Mercado, S. Schroff, K. Robinson, P. Schumacker, L. Alger, Q. Niu, and J. Solway.** Detection of individual tracheal myocyte contraction using atomic force microscopy (Abstract). *Am. J. Respir. Crit. Care Med*. 153: A168, 1996.
16. **Janssen, L. J., and S. M. Sims.** Emptying and refilling of Ca^{2+} store in tracheal myocytes as indicated by ACh-evoked currents and contraction. *Am. J. Physiol*. 265 (*Cell Physiol*. 34): C877–C886, 1993.
17. **Lau, C. L., and S. Chacko.** Identification of two types of smooth muscle cells from rabbit urinary bladder. *Tissue Cell* 28: 339–355, 1996.
18. **Ma, X. F., Y. Wang, and N. L. Stephens.** Serum deprivation induces a unique hypercontractile phenotype of cultured smooth muscle cells. *Am. J. Physiol*. 274 (*Cell Physiol*. 43): C1206–C1214, 1998.
19. **Majack, R. A., N. A. Grieshaber, C. L. Cook, M. C. M. Weiser, R. C. McFall, S. S. Grieshaber, M. A. Reidy, and C. F. Reilly.** Smooth muscle cells isolated from the neointima after vascular injury exhibit altered responses to platelet-derived growth factor and other stimuli. *J. Cell. Physiol*. 167: 106–112, 1996.
20. **Mitchell, R. W., and A. J. Halayko.** Airway smooth muscle structure. In: *Asthma,* edited by P. J. Barnes, M. W. Grunstein, A. R. Leff, and A. J. Woolcock. Philadelphia, PA: Lippincott-Raven, 1997, p. 733–758.
21. **Mitchell, R. W., A. J. Halayko, J. Solway, and M. E. Wylam.** Induction of functional muscarinic receptor responsiveness in cultured airway smooth muscle myocytes (Abstract). *Am. J. Respir. Crit. Care Med*. 157: A655, 1998.
22. **Owens, G.** Regulation of differentiation of vascular smooth muscle cells. *Physiol. Rev*. 75: 487–517, 1995.
23. **Panettieri, R. A., R. K. Murray, L. R. DePalo, P. A. Yadvish, and M. I. Kotlikoff.** A human airway smooth muscle cell line that retains physiological responsiveness. *Am. J. Physiol*. 256 (*Cell Physiol*. 25): C329–C335, 1989.
24. **Ross, R.** The pathogenesis of atherosclerosis: a perspective for the 1990s. *Nature* 362: 801–809, 1993.
25. **Shore, S. A., J. Laporte, I. P. Hall, E. Hardy, and R. A. Panettieri, Jr.** Effect of IL-1β on responses of cultured human airway smooth muscle cells to bronchodilator agonists. *Am. J. Respir. Cell Mol. Biol*. 16: 702–712, 1997.
26. **Schuger, L., A. P. N. Skubitz, J. Zhang, L. Sorokin, and L. He.** Laminin α1 chain synthesis in the mouse developing lung: requirement for epithelial-mesenchymal contact and possible role in bronchial smooth muscle development. *J. Cell Biol*. 139: 553–562, 1997.
27. **Schuger, L., P. Yurchenko, N. Relan, and Y. Yang.** Laminin fragment E4 inhibition studies: basement membrane assembly and embryonic lung epithelial cell polarization requires laminin polymerization. *Int. J. Dev. Biol*. 42: 217–220, 1998.
28. **Smith, P. G., R. Garcia, and L. Krogerman.** Strain reorganizes focal adhesions and cytoskeleton in cultured airway smooth muscle cells. *Exp. Cell Res*. 232: 127–136, 1997.
29. **Smith, P. G., R. Garcia, and L. Krogerman.** Mechanical strain increases protein tyrosine phosphorylation in airway smooth muscle cells. *Exp. Cell Res*. 239: 353–360, 1998.
30. **Smith, P. G., R. Moreno, and M. Ikebe.** Strain increases airway smooth muscle contractile and cytoskeletal protein in vitro. *Am. J. Physiol*. 272 (*Lung Cell. Mol. Physiol*. 16): L20–L27, 1997.
31. **Thyberg, J., and A. Hultgardh-Nilsson.** Fibronectin and the basement membrane components laminin and collagen type IV influence the phenotypic properties of subcultured rat aortic smooth muscle cells differentially. *Cell Tissue Res*. 276: 263–271, 1994.
32. **Thyberg, J., J. Roy, P. K. Tran, K. Blomgren, A. Dumitrescu, and A. Hedin.** Expression of caveolae on the surface of rat arterial smooth muscle cells is dependent on the phenotypic state of the cells. *Lab. Invest*. 77: 93–101, 1997.
33. **Tom-Moy, M., J. M. Madison, C. A. Jones, P. de Lanerolle, and J. K. Brown.** Morphologic characterization of cultured smooth muscle cells isolated from the tracheas of adult dogs. *Anat. Rec*. 218: 313–328, 1987.
34. **Vincent, S. G., P. R. Cunningham, N. L. Stephens, A. J. Halayko, and J. T. Fisher.** Quantitative densitometry of proteins by an HP Scanjet scanner and Scanplot software. *Electrophoresis* 18: 67–71, 1997.
35. **Xiong, W., R. G. Pestell, G. Watanabe, J. Li, M. R. Rosner, and M. B. Hershenson.** Cyclin D1 is required for S phase traversal in bovine tracheal myocytes. *Am. J. Physiol*. 272 (*Lung Cell. Mol. Physiol*. 16): L1205–L1210, 1997.
36. **Yang, C. M., S.-P. Chou, T.-C. Sung, and H.-J. Chien.** Regulation of functional muscarinic receptor expression in tracheal smooth muscle cells. *Am. J. Physiol*. 261 (*Cell Physiol*. 30): C1123–C1129, 1991.